J Seismol (2012) 16:709–720
DOI 10.1007/s10950-012-9300-0

ORIGINAL ARTICLE

Investigation of ground rotational motions caused by direct and scattered P-waves from the 4 March 2008 TAIGER explosion experiment

Nguyen Dinh Pham · Bor-Shouh Huang · Chin-Jen Lin · Tuan-Minh Vu · Ngoc-Anh Tran

Received: 21 August 2011 / Accepted: 13 March 2012 / Published online: 4 April 2012

Abstract High-frequency rotational motions of P-waves and coda waves were analysed using rotation rate sensors and strong motion array data from the 4 March 2008 TAiwan Integrated GEodynamics Research (TAIGER) explosion experiment in northeastern Taiwan. Theoretical and observational investigations focussed on the effects of this experiment on the free surface. The main goal of this study was to explore possible applications of combined measurements of artificial explosion-derived translational and rotational motions. Also investigated was the consistent ground rotation observed directly by rotation rate sensors and derived using translational seismic arrays. Common near-source high-frequency rotational motion observations and array-recorded translational motions from one shallow borehole explosion are analysed in this study. Using a half-space assumption of plane P-wave propagation across the recording site, we conclude that: (1) rotational motions induced by direct P-waves interacting with a free surface in theory can be used to estimate wave radial direction, velocity and anisotropic properties; (2) rotational motions derived from scattering are predominant among the observed rotations during the TAIGER explosion experiments and allow us to image the heterogeneous structure of the medium at the investigated site; and (3) rotation sensor measurements undertaken during TAIGER explosion experiments may be affected by cross-axis sensitivities, which need to be considered when using the data obtained during these experiments.

Keywords Rotational motion · P wave · Wave radial direction · Wave velocity · Anisotropy · Scattering

N. D. Pham (✉) · T.-M. Vu · N.-A. Tran
Institute of Geophysics,
Vietnam Academy of Science and Technology,
18 Hoang Quoc Viet, Nghia Do, Cau Giay,
Hanoi, Vietnam
e-mail: nguyendp@igp-vast.vn

N. D. Pham
e-mail: ndpseis@googlemail.com

B.-S. Huang · C.-J. Lin
Institute of Earth Sciences, Academia Sinica,
128, Sec. 2, Academia Road, Nangang,
Taipei 115, Taiwan, Republic of China

1 Introduction

A number of new aspects of rotational motion induced by earthquakes and explosions have emerged as an active branch of seismological research (Lee et al. 2009a, b). Though theoretical ground rotational motions have been known for a number of years, the effects of these rotation motions were thought to be insignificant and therefore would have negligible effects on ground motions (Gutenberg 1927; Richter 1958; Båth 1979; Aki and Richard 1980). Recently, during analysis of recorded strong ground motions, it was found that the recording of translational motions could be contaminated by ground rotational effects. For example, if three-component translational seismograms alone cannot exclude the possibility of observed ground tilts, rotational signals should be measured to correct this effect (Trifunac and Todorovska 2001; Graizer 2005, 2006; Pillet and Virieux 2007).

Ground rotations are usually inferred using observations from dense seismic arrays (Huang 2003; Suryanto et al. 2006; Langston et al. 2009). The array processing technique known as wave gradiometry was developed using the spatial gradient of the seismic wave field in order to determine the attributes of propagating seismic waves (Langston 2007a, b; Liang and Langston 2009). Wave gradiometry has successfully been used to analyse rotational motion using data obtained from seismic arrays (Langston and Liang 2008; Langston et al. 2009). In addition, the renewed seismological interest in ground rotation has arisen because of the development of instruments to measure rotations and because of recent developments in the consistent observation of rotational motions across broad ranges of frequency and distance (McLeod et al. 1998; Pancha et al. 2000; Schreiber et al. 2005, 2006). Combined high-quality measurements of translational and rotational motions at one site allow the extraction of additional information (e.g. phase velocity; Igel et al. 2005; Cochard et al. 2006) that otherwise can only be obtained by using additional high-accuracy strain or translational array measurements (Igel et al. 2007).

Recent studies have attempted to extend this analytical approach to various wave types. Igel et al. (2005, 2007) and Lin et al. (2011) analysed Love and Rayleigh wave phase velocities determined for teleseismic events and established that the shear wave velocity of the surface layer might be extracted from the recordings of both rotational and translational motions from a single station. Pham et al. (2009a) used analysis of P-wave coda signals of translational and rotational motion about a vertical axis caused by distant strong earthquakes to extract the scattering properties of the Earth's crust. In addition, Fitchner and Igel (2009) and Bernauer et al. (2009) theoretically determined that shear wave structures could be inverted using multicomponent rotational and translational motion point measurements without travel time information. Furthermore, whilst investigating the presence of rotational motions induced by P-waves in homogeneous anisotropic media, Pham et al. (2010) indicated that rotational motions contain additional information about the anisotropy of the material and that joint measurement of P-wave-induced translational and rotational motion might provide constraints on the anisotropic parameters of the propagation media.

Building on this previous research, here, we consider the free surface conditions of wave propagation. We extend on the work of previous investigations of rotational motion induced by P-waves (Pham et al. 2009a, 2010) that focussed on wave propagation over teleseismic distances and in full-space cases. Our analysis reports results from direct and scattering waves from near-source high-frequency waves. This study has been made possible by the pioneering six-degree-of-freedom observations undertaken in northeastern Taiwan during the TAiwan Integrated GEodynamics Research (TAIGER) explosion experiments (Lin et al. 2009). This study was initially based on the theoretical approach of Li et al. (2001), but focuses on determining a more convenient relationship between rotation rates and translational accelerations. The main goal was to explore the application of combined recordings of rotational and translational motion on a free surface, as measured by the TAIGER explosion experiments, and to extract additional information from these measurements. Translational and rotational ground motion seismograms, derived from 3D numerical simulations and field observations, are processed and analysed to examine the propagation behaviour of P-waves and P-wave coda induced by both the free surface of the ground and the heterogeneity of the propagation media. We finally discuss the possible applications of these measurement techniques and consider aspects of this approach that remain unclear and require further study.

2 Data

In 2005, the TAIGER experiment, an international project that sought to study the Taiwan orogeny, was performed to test existing geodynamical models and to develop new models based on geophysical imaging, earthquake recording and subsequent geodynamic analysis (Wu et al. 2009; Okaya et al. 2009). In early 2008, dense seismic refraction and wide-angle reflection explosion experiments were successfully conducted along two E–W profiles across northern and southern Taiwan. On 4 March 2008, a shallow borehole explosion, at a depth of 80 m and named N3P, was conducted at 17:01 UTC. Seismic sources were exploded with a charge of 3,000 kg at 24.5782° N, 121.4795° E, and this was one of a series of explosions along the northern Taiwan profile.

During this explosion, strong translational motion instruments and rotation sensors were deployed in a seismic array to measure ground rotation near the explosion source (Lin et al. 2009). This dense seismic array was equipped with 11 strong motion seismometers and was about 25 m in size. In the centre of the array, five three-component R-1 rotation sensors were installed in addition to translation sensors with epicentral distances of about 500 m. The observations made by these instruments form the central part of this study. In addition, we employed translation and rotation signals from five common recording sites (sites N03, N05, N06, N07 and N09 in Lin et al. 2009; the same nomenclature is used here as in this previous study). All translational sensors (TSA-100S) used were Metrozet triaxial accelerometers (Metrozet 2007) with an amplitude response that is flat from direct current to 200 Hz. All rotational sensors (R-1) used during the study were eentec triaxial rotational velocity sensors (eentec 2008) with a bandwidth of 0.05–20 Hz. For details on the sensors, see Lin et al. (2009).

3 Fundamental theory

An incident plane P-wave with a frequency ω that propagates in the (x_1, x_3) plane of a homogeneous isotropic medium with $-x_3$ and $+x_1$ directions; when it impinges on a free surface, it creates two other reflected waves immediately after encountering the surface (Fig. 4.1.a, p. 117 in Lay and Wallace 1995). The displacements (u_1 and u_3) at the free surface can be determined as follows (Lay and Wallace 1995):

$$u_1 = i\omega\left(p\phi_I + p\phi_R - \eta_\beta\psi\right), \tag{1}$$

$$u_3 = i\omega(-\eta_\alpha\phi_I + \eta_\alpha\phi_R + p\psi). \tag{2}$$

where ϕ_I, ϕ_R and ψ are the potentials of waves defined by

$$\phi_I = A\exp[i\omega(px_1 - \eta_\alpha x_3 - t)], \tag{3}$$

$$\phi_R = B\exp[i\omega(px_1 + \eta_\alpha x_3 - t)], \tag{4}$$

$$\psi = Cexp\left[i\omega\left(px_1 + \eta_\beta x_3 - t\right)\right], \tag{5}$$

and

$$\eta_\alpha = \sqrt{\frac{1}{\alpha^2} - p^2} = \frac{\cos i_1}{\alpha}, \eta_\beta = \sqrt{\frac{1}{\beta^2} - p^2} = \frac{\cos j_2}{\beta}. \tag{6}$$

Herein, p is the seismic ray parameter, or horizontal slowness; α and β are the P- and S-wave velocities, respectively; i_1 is the incident angle of the P-wave; and j_2 is the angle of SV-wave (S-wave polarized in the vertical plane) reflection.

Following Cochard et al. (2006), the corresponding rotational motions can be calculated as follows:

$$\Omega_1 = \frac{\partial u_3}{\partial x_2} = 0, \tag{7}$$

$$\Omega_2 = -\frac{\partial u_3}{\partial x_1} = -i\omega p u_3, \tag{8}$$

and

$$\Omega_3 = \frac{1}{2}\left(\frac{\partial u_1}{\partial x_2} - \frac{\partial u_2}{\partial x_1}\right) = 0. \tag{9}$$

Equations 7–9 indicate that, on a free surface, direct P-waves do generate rotational motions, but around the transverse axis only. Along the vertical and radial axes, the rotational motions are zero.

Comparing the rotation rate about the transverse axis given as $\dot{\Omega}_2$, as inferred from Eq. 8, with the translational acceleration of the particle motions along the vertical axis, given as $\ddot{u}_3$ and as inferred from Eq. 2, we have:

$$\frac{\ddot{u}_3}{\dot{\Omega}_2} = \frac{1}{p}. \tag{10}$$

Equation 10 reveals that the vertical component of translational acceleration and the transverse component of the rotation rate caused by P-waves interacting with the free surface are in phase, and the amplitudes of the two signals are scaled by the inverse seismic ray parameter. This also implies that the apparent velocity

($1/p$) of a P-wave can be determined if its transverse rotation rate and vertical translational acceleration on the free surface are measured with a sufficiently high signal-to-noise ratio. Furthermore, these measurements may allow us to infer the physical velocities (i.e. P- or S-wave velocities) because the incident angle of the P-wave, or the reflection angle of the SV wave, in theory, can be determined, such as (see Li et al. 2001):

$$\frac{u_1}{u_3} = -tg(2j_2). \tag{11}$$

In real observations, rotational motions can be directly measured using rotation sensors; however, rotation motions can also be determined from spatial derivatives of translational motions measured by a seismic array. Thus, one can obtain Eqs. 7–10 by using the definition of wave spatial gradients expressed by Eq. 3, as presented in Langston and Liang (2008). Equation 8 in Langston (2007a), for the spatial gradient of a seismic plane wave, is another expression of Eq. 10 in this study.

In other cases, in a (x_1, x_2, x_3) Cartesian system, and assuming plane shear wave propagation with velocity $c=\omega/k$ in the plan consisted of vertical x_3 direction and with polarization in the x_2 direction, the translational displacements, velocities and accelerations of the plane shear waves can be expressed as follows:

$$\mathbf{u} = [0, u_2(x_3, t), 0] = [0, f(kx_3 - \omega t), 0], \tag{12}$$

$$\mathbf{v} = [0, \dot{u}_2(x_3, t), 0] = [0, -\omega f(kx_3 - \omega t), 0], \tag{13}$$

$$\mathbf{a} = [0, \ddot{u}_2(x_3, t), 0] = \left[0, \omega^2 f(kx_3 - \omega t), 0\right]. \tag{14}$$

The corresponding rotation rates of the plane shear waves can be calculated using:

$$\dot{\Omega} = \frac{1}{2}\nabla \times [0, \dot{u}_2, 0] = \left[-\frac{1}{2}\frac{\omega^2}{c} f(kx_3 - \omega t), 0, 0\right]. \tag{15}$$

Equations 14 and 15 demonstrate that the x_1 component of the rotation rate and the x_2 component of translational acceleration have the same waveform, and their amplitudes should therefore both scale proportionally to double the velocity. This result is similar to those obtained by Igel et al. (2005), Cochard et al. (2006) and Igel et al. (2007) for plane transversely polarized waves propagating along a horizontal plane. These theoretical results suggest that variations in cross-correlation coefficients between the (1) radial rotation rate and translational acceleration on the transverse–vertical plane and the (2) vertical rotation rate and translational acceleration on the transverse–radial plane may provide information on the origins of S-wave energy.

In summary, the results presented here suggest theoretically that (1) the velocities of waves in the subsurface can be extracted using P-wave-derived translational and rotational motion, multicomponent point measurements, on a free surface; (2) P-wave radial direction can be estimated by searching the back-azimuth for the maximum cross-correlation between the vertical component of translational acceleration and the transverse component of the rotational rate, and for the minimum amplitude of the radial component of the rotation rate in the P-wave time window; and (3) structural properties near the receiver (e.g. scattering, anisotropy) can be determined from rotational signals about both the vertical and radial axes if these signals are obtained because the contribution of direct P-waves to these rotational components is zero in homogeneous isotropic media.

4 Analysis and results

To address the points outlined above, we process and analyse both synthetic and observed P-wave-derived free surface rotational and translational seismograms. We firstly use synthetic seismograms generated by a 3D earth model numerical simulation. Here, we aimed to determine whether translational and rotational signal waveforms caused by direct P-waves were similar. The model and numerical simulation method employed here provided six-component seismograms as described by Igel et al. (2005). Six-component synthetic teleseismic seismograms were computed for the Wettzell seismic station in southeast Germany using both the 25 September 2003 M8.1 Tokachi-Oki earthquake and the 7 February 2004 M7.5 Irian Jaya earthquake seismic events. To ensure that the waveforms generated were accurate and to fulfil the plane wave assumption, we filtered synthetic waveforms between periods of 20 and 100 s. Seismograms were rotated to align with the vertical, transverse and radial components (see Pham et al. 2009b and Pham et al. 2010 for the way to do axis transformation of rotational components); then, the transverse rotation rate was superimposed on the vertical translational acceleration (Fig. 1). The excellent fit of superposition signal waveforms immediately after the first P-wave arrival (Fig. 1c, g) confirms the relationship given in Eq. 10. Moreover, the absence of rotational signals about the vertical and radial axes in the narrow time windows corresponding to the first wave arrivals (Fig. 1a, b, from 715 to about 735 s for the Tokachi-Oki event; Fig. 1e, f, from 1,115 to about 1,135 s for the Irian Jaya event) verifies the relationships outlined in Eqs. 7 and 9.

Based on this numerical modelling, we tested whether the back-azimuth could be determined from the available seismograms using Eq. 10. During this part of the study, the following steps were followed: (1) random noise with an amplitude of 10 % of the signal peak was added to the seismograms in order to simulate real conditions; (2) axis transformations for available north–south and east–west rotation rate

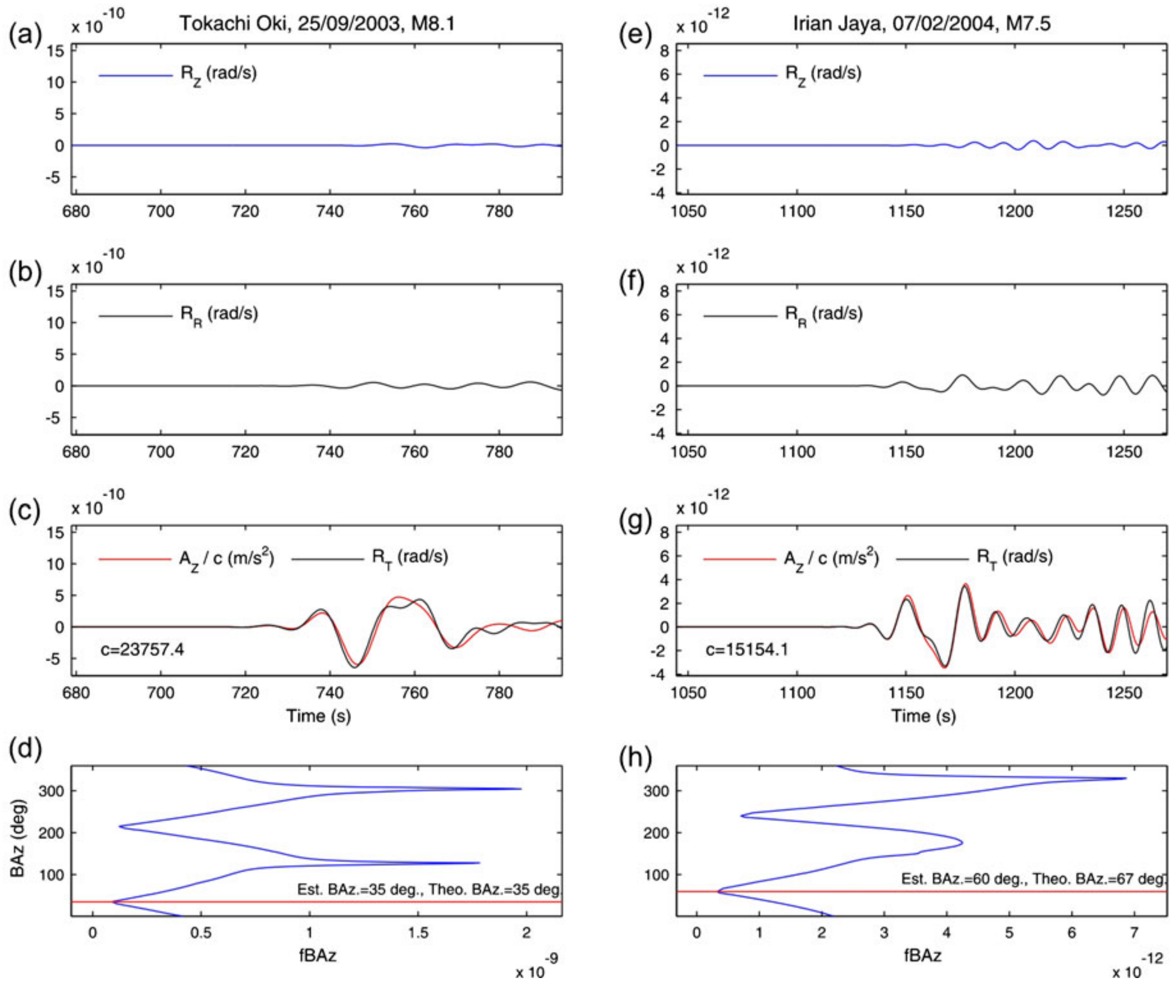

Fig. 1 **a**–**c**, **e**–**g** Three-dimensional modelling of narrow-time-window seismograms from the Wettzell station, southeast Germany, of the first arrival waves for (*1*) the Tokachi-Oki earthquake on 25 September 2003 (M=8.1) and (2) the Irian Jaya earthquake on 7 February 2004 (M=7.5). Here, R_Z, R_R and R_T are the vertical, radial and transverse components of the rotation rate, respectively, and A_Z is the vertical translational acceleration. *Blue curves* in (**d**) and (**h**) represent variations in the product of the peak amplitude of the radial rotation rate and the inverse of cross-correlation coefficients between A_Z and R_T. The coefficients are determined assuming the back-azimuth (denoted as *BAz*) in narrow time windows corresponding to the first P-wave arrivals (from 710 to 760 s for the Tokachi-Oki event; from 1,110 to 1,160 s for the Irian Jaya event). This product is abbreviated to *fBAz*; the *horizontal red line* is plotted at the BAz value that corresponds with the minimum value of fBAz

components were undertaken, assuming that transverse and radial components had different back-azimuths (which were varied between 1° and 360°); (3) cross-correlation coefficients between the vertical component of translational acceleration and the transverse component of rotation rate were calculated for a narrow time window that corresponded to the first P-wave arrival (from 710 to 760 s for the Tokachi-Oki event; from 1,110 to 1,160 s for the Irian Jaya event) as a function of the back-azimuth; and (4) we identified back-azimuths corresponding to minimum values for the product of the peak amplitude of the assumed radial rotation rate (in the narrow time window outlined above) and the inverse of the calculated cross-correlation coefficients. The results presented in Fig. 1d, h indicate that the estimated back-azimuths are almost coincident with the theoretical ones; the error of 7° between the estimated and theoretical back-azimuths for the Irian Jaya event may originate from either random noise or the presence of weak scattering signals within the available synthetic rotation rates. This method is one potential procedure with which to enable the determination of the wave radial direction using multicomponent point measurements, as demonstrated successfully in this study.

In addition to the modelling outlined above, we used a similar methodology applied to six-degree-of-freedom observations obtained during the TAIGER explosions. The observed data were converted to theoretical transverse, radial and vertical directions, hereby defined as *X*, *Y* and *Z* components, respectively. To satisfy the plane-wave assumption, we use seismograms obtained for the N3P explosion from stations N03, N05, N06, N07 and N09 (with an epicentral distance of about 500 m) and only consider frequencies above 10 Hz. We also use a second-order Butterworth filter to restrict the observed waveforms to frequencies between 10 and 12 Hz. The results of this filtering are presented in narrow time windows corresponding to the first P-wave arrival times (Fig. 2).

To determine incident P-wave azimuths, we apply the technique used previously with the synthetic data to estimate the radial wave direction. During these estimations, a time window from 7.9 to 8.04 s was used. We rotated *X*- and *Y*-axes by 1°–360° clockwise around the *Z*-axis and identified axis transformation angles that corresponded to the minimum values of the product of (a) the peak amplitude of the rotation rate about a new *Y*-axis (new radial) and (b) the inverse of the cross-correlation coefficients between the vertical translational acceleration and the rotation rate about a new *X*-axis (new transverse). The result is shown in the bottom panels of Fig. 2. Our results contrast with those of Langston et al. (2009) in that P-waves travel at an off-azimuth angle of 35° from the theoretical radial direction; in addition, station N03 gave the most consistent results. The new transverse and radial rotation rates obtained for the five stations used during this study are given in rows (b) and (c) of Fig. 2 and are shown as red traces. It is clear that, although the transverse rotation rate and the vertical translational acceleration for the first P-wave have the same waveforms as expected from theoretical calculations, significant rotational signals about both radial and vertical axes are observed within the original (*X*, *Y*, *Z*) and the new radial–transverse systems. The origins of these unexpected signals are discussed in the following section.

During the TAIGER explosion experiments, strong translational motion instruments were deployed as a seismic array. Rotational motions can be determined using translational ground motions (Langston et al. 2009). To examine whether rotational signals about a radial axis, in the time window defined by the arrival of the first P-wave, are influenced by cross-axis sensitivities, we calculated the rotational signals from the translational signals recorded by accelerometers at stations N03, N05, N06, N07 and N09 using the method proposed by Spudich and Fletcher (2008). These calculated rotations are hereby called ‘array-derived rotations’. We also note that in the calculations to derive these rotations, the effects of tilt and translation upon the accelerometer can be neglected if the assumption of uniform strain is valid (Lin et al. 2012). Furthermore, during the determination of the spatial gradient of the array using a finite difference approximation, errors increase with frequency. The maximum frequency of the obtained signals is defined by f_{max}= 0.123c/h for errors of 10 % or less, where c is wave velocity and h is array spacing (see Langston 2007a). As the averaged array spacing is ~10 m, if we assume that c=1,000 m/s, the f_{max} of the array-derived rotations is about 12.3 Hz. Given this, we filtered the array-derived rotational data to remove frequencies outside of a 10- to 12-Hz band, as shown in Fig. 3. Immediately after the arrival of the first P-wave, the rates of transverse rotation and vertical translational acceleration have the same waveforms, and the vertical

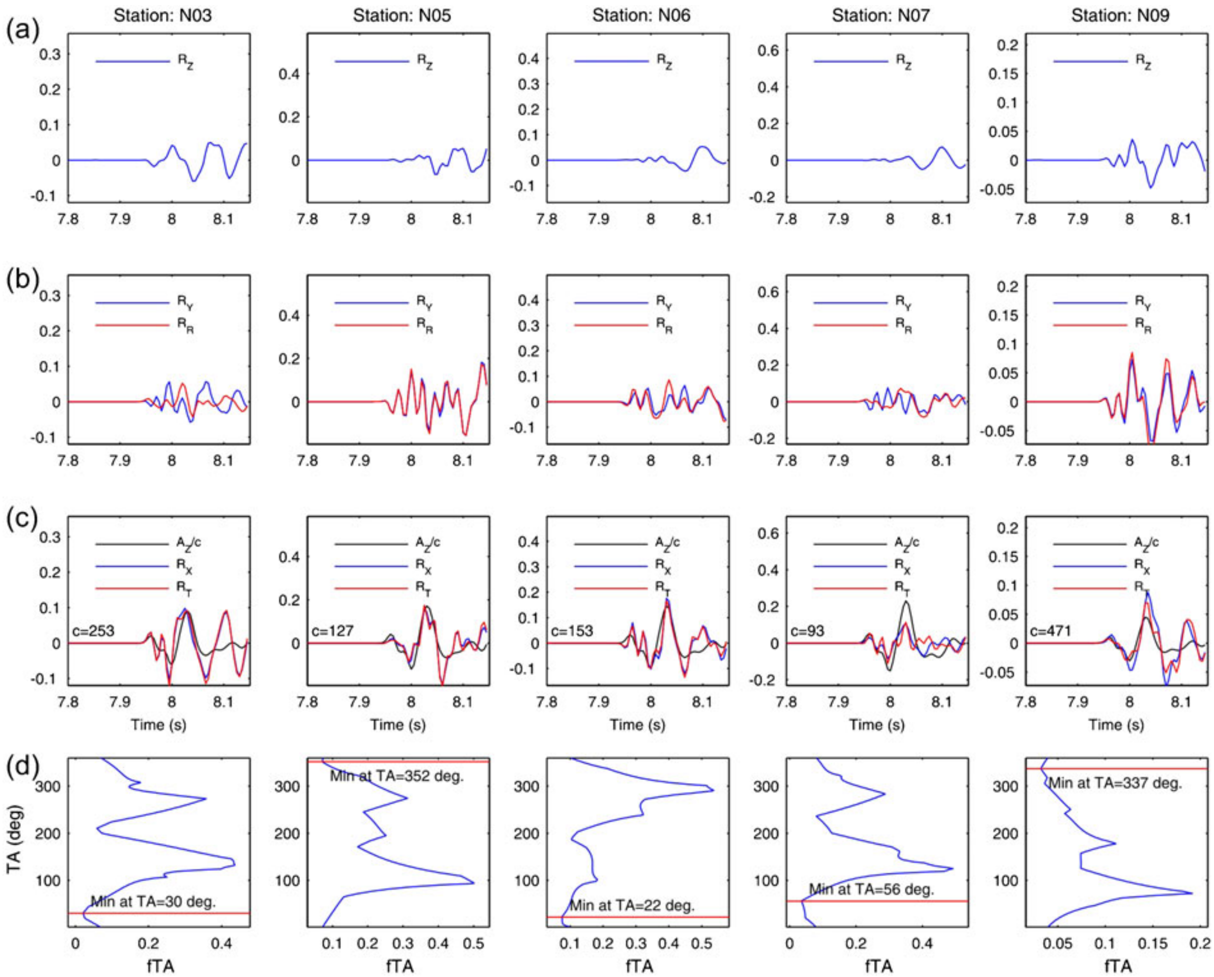

Fig. 2 *Panels* in (**a**–**c**) *Blue* and *black traces* show the observed signals of the TAIGER N3P explosion across a narrow time window corresponding to the first wave arrivals. Rotation rates were recorded by the R-1 sensor and translational accelerations were measured by the Metrozet TSA-100S instrument. *Red traces* indicate the estimated transverse–radial axis rotational signals. *Panels* in (**d**) *Blue curves* indicate variations in the value of the product of the peak amplitude of the radial rotation rate and the inverse of the cross-correlation coefficients between transverse rotation rate and vertical acceleration as a function of the axis transformation angle (*TA*) between 7.9 and 8.04 s. The product is abbreviated to *fTA*; the *horizontal red line* is plotted at the TA that corresponds to the minimum fTA value. Vertical R_Z, radial R_Y, R_R and transverse R_X and R_T components of the rotation rates are in milliradian per second; the vertical component of the translational acceleration A_Z is in centimetres per square second. The signals are band-pass-filtered using a 10- to 12-Hz second-order Butterworth filter

component has almost no rotational signal. In comparison, though the rotation signal about the radial axis in the narrow time window derived by the arrival of the first P-wave is weak, it is still recognisable and should be considered as anisotropy-induced, as proposed by Pham et al. (2010).

To test the possible effects of anisotropy on the recorded ground rotations, we used a simple transverse isotropic media. Estimations and the discussions below also considered a transverse isotropic media; investigations with other types of anisotropy were not considered here. We follow the method presented by Pham et al. (2010) to estimate the maximum rotation rate generated by P-wave propagation in transverse isotropic media. The amplitude of the P-wave used in this estimation equalled the maximum amplitude of P-waves with a peak ground displacement (PGD) of 126×10^{-6} m, as obtained at stations N03, N05, N06, N07 and N09 during the N3P explosion experiment. We used a frequency of 12 Hz. The estimated maximum rotation rates at different levels of anisotropy are given in Fig. 4, which indicate that anisotropy may contribute

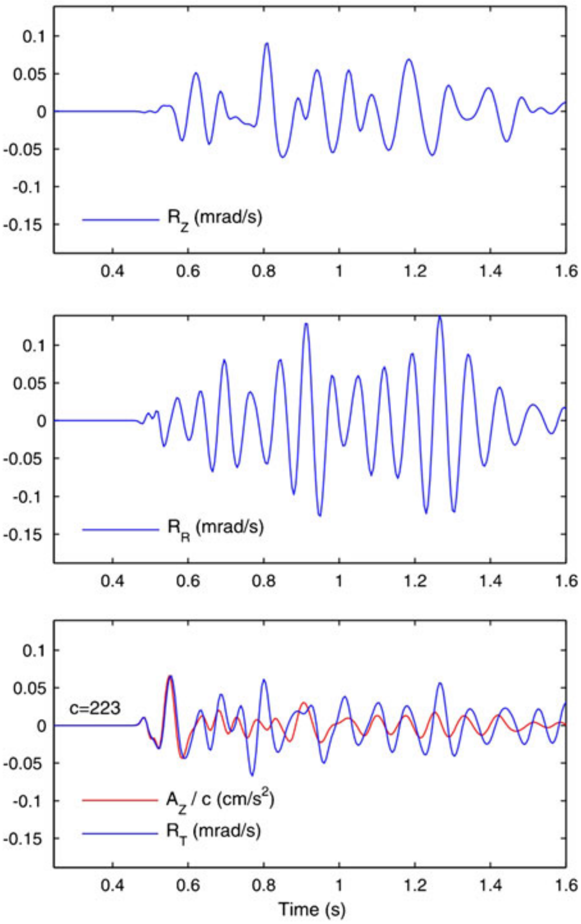

Fig. 3 Vertical R_Z (*top*), radial R_R (*middle*) and transverse R_T (*bottom*, *blue*) components of the array-derived rotation rates (in milliradian per second) and observed translational acceleration along the vertical axis A_Z (*bottom*, *red*, in centimetres per square second) at station N06 during the TAIGER N3P explosion in northeastern Taiwan. All signals are band-pass-filtered using a 10- to 12-Hz second-order Butterworth filter

amplitude signals of >0.02 mrad/s to measurements of the total direct P-wave-induced rotational rate. This is a significant contribution in comparison with the observed peak amplitude of about 0.2 mrad/s of rotational signal around the transverse axis for the first P-wave arrival (Figs. 2 and 3).

Even given this, by intuition, one can easily recognise in Fig. 3 that, amongst the array-derived rotations, the radial component is predominant and the maximum amplitudes appear in the P-coda time window. Considering the results presented in Section 3 above, it is possible to infer that the observed rotational signals about the radial and vertical axes in the P-coda are caused by P- and S-wave scattering (Pham et al. 2009a). Herein, we follow Pham et al. (2009a) in using the correlation between the rotation rate and translational acceleration to investigate this phenomenon. Accelerations on the vertical–transverse plane were axis-transformed by rotating 1°–180° around the radial axis (i.e. covering half of the space), and we then examined the maximum normalised cross-correlation coefficients between the translational acceleration along the new transverse axis and the radial rotation rate in sliding time windows. The sliding time window lengths were twice the maximum period of the signals (0.2 s) with a sliding step of 1/30 of the size of the sliding window length.

Figure 5d shows the results for the observed array data obtained during the TAIGER explosion experiments. High correlation coefficients are randomly distributed within both axis transformation angle and time, suggesting that the media around the investigated site have a heterogeneous structure. A rough distribution of the medium velocities for the vertical–transverse plane can be obtained by simply taking half of the ratio of the translational acceleration and the rotation rate where the normalised cross-correlation coefficient between the two is ≥0.8 (Fig. 5e). Similarly, we undertook axis transformations for radial–transverse plane accelerations by rotation between 1° and 360° clockwise around a vertical axis in order to ensure that all directions of incoming waves in the horizontal plane were covered. We then examined the maximum normalised cross-correlation coefficients between the translational acceleration along the new transverse axis and the vertical rotation rate, within sliding time windows. The obtained distribution of these correlation coefficients and the horizontal plane velocities from the observed array data obtained during the TAIGER explosion experiments are presented in Fig. 5i, j. These results compare well with the description of the investigation site documented by Lin et al. (2009) in that the ground around the central array is alluvium with a mixture of mud and stones, a medium which inherently has a high scattering effect on any waves passing through it. This result suggests that the proposed approach is useful for investigating random structures within the wave propagation medium.

5 Discussions and conclusions

The seismological observations obtained in northeastern Taiwan during the TAIGER explosion experiments

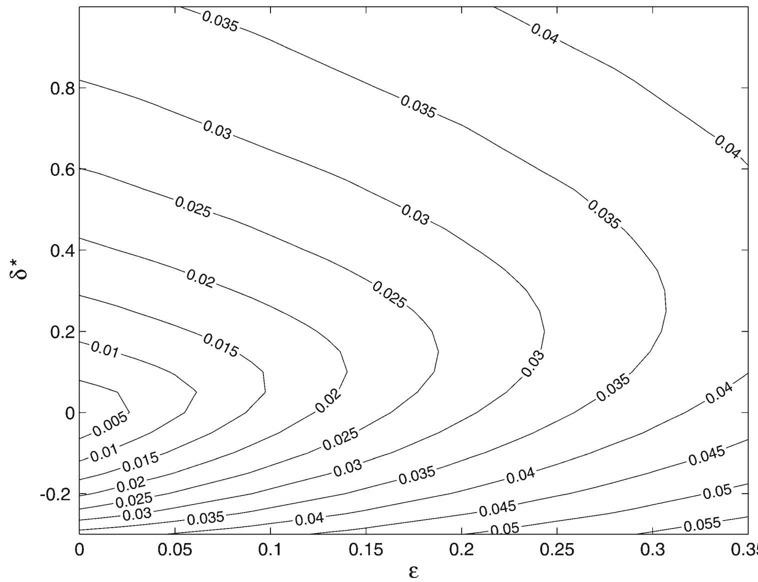

Fig. 4 Maximum rotation rates (in milliradian per second) induced by plane P-waves of frequency 12 Hz as a function of anisotropy level, where PGD=126× 10–6 m, which is the same as the strongest P-waves caused by the TAIGER N3P explosion in northeastern Taiwan at stations N03, N05, N06, N07, or N09. The Thomsen parameters ε and δ^* characterize the strength of the anisotropy, assuming transverse isotropic media

provide several pioneering six-degree-of-freedom point measurements, identical to deploying a dense seismic array (Lin et al. 2009). In this study, we extended the research undertaken on data obtained from the TAIGER experiments into rotational motions induced by near-source high-frequency P-waves in order to examine the scattering and anisotropy of rotational motions. This scattering and anisotropy has previously been reported by Pham et al. (2009a) and (2010) for scattering of long-period signals at teleseismic distances and within homogeneous anisotropic media, respectively. Using rotational and translational motions observed at a single site and using theoretical results to guide our investigative methodology, we considered the following possible approaches: (a) using the amplitude ratio between vertical acceleration and transverse rotation rates in the time window defined by the first arrival of P-waves to estimate wave velocities; (b) using the azimuth-dependent character of radial and transverse rotation rates of P-waves to determine the wave arrival direction; (c) investigating the anisotropy by exploiting rotational signals about vertical and radial axes in the time window defined by the first arrival of P-waves; and (d) identifying the heterogeneous properties using P–S scattering rotations about both the vertical and radial axes. The obtained results indicate that the estimation of wave radial direction using P-wave rotational motions on a free surface can be successfully undertaken, and wave scattering is a dominant phenomenon within the data obtained during TAIGER explosion experiments.

As shown in Fig. 2c, the superposition of transverse rotation rates (R_X, blue trace in the figure) and vertical translational accelerations (A_Z, black trace) indicates that, for the arrival of the first P-wave, the waveforms of these two signals are similar, as suggested by theoretical calculation. In comparison, and different from the results of numerical modelling (Fig. 1), significant rotational signals about both radial (R_Y) and vertical (R_Z) axes are observed after the arrival of the first P-wave (shown by blue traces in Fig. 2a, b). There are three possible explanations for these unexpected observations: (1) wave propagation direction—the presence of a complicated 3D structure means that the first P-waves do not arrive at receivers in radial directions that entirely agree with theoretical models, thus creating rotational signals about the *X*-axis; (2) influence of cross-axis sensitivity—the R-1 instrument may record a signal polluted by translation and/or cross-axis rotation, as indicated by Nigbor et al. (2009); (3) anisotropy effects—as suggested by Pham et al. (2010), the propagation of P-waves in anisotropic media generates rotational motions, and this may contribute to our observations.

From the data presented here, we have shown that rotational motions were directly measured using rotation sensors; however, rotational motions can also be determined using spatial derivatives of translational motions from a seismic array. This study also provided an opportunity to test the performance of R-1 rotation rate sensors during rotation measurement. Array-derived rotations (Fig. 3) reveal that the weak rotational

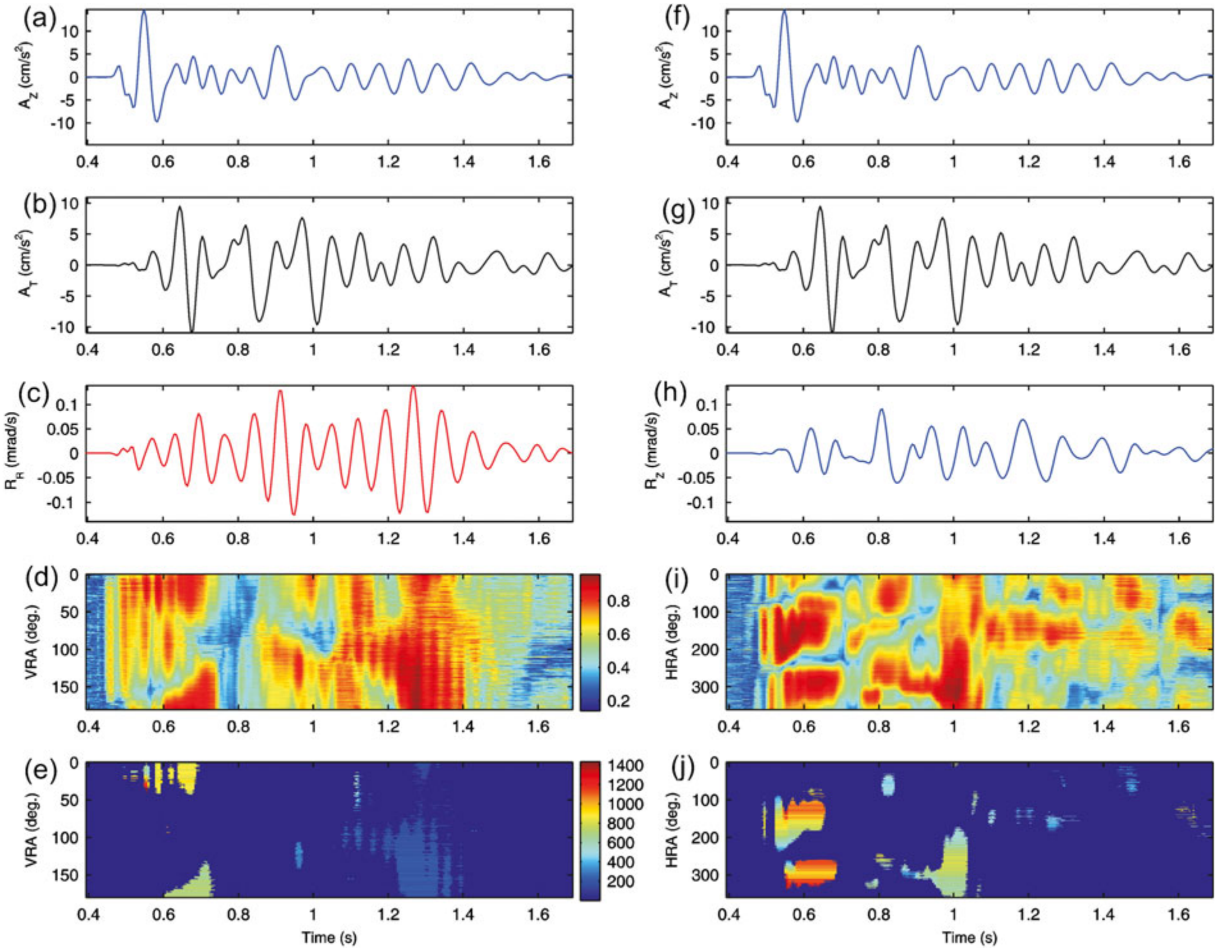

Fig. 5 **a**–**c**, **f**–**h** Observed translational accelerations and array-derived rotation rates obtained at station N06 for the TAIGER N3P explosion in northeastern Taiwan. **d** Variation in cross-correlation coefficients between transverse acceleration A_T and radial rotation rate R_R as a function of time and axis transformation angle of A_T in the transverse–vertical plane; angle is denoted as *VRA*. **e** Distribution of the medium velocities in the transverse–vertical plane. Velocities were determined by halving the A_T/R_R ratio where the normalised cross-correlation coefficient is ≥0.8. **i** Variation in cross-correlation coefficients between transverse acceleration A_T and vertical rotation rate R_Z as a function of time and axis transformation angle of A_T in the transverse–radial plane. This angle is denoted as *HRA*. **j** Distribution of the medium transverse–radial plane velocities obtained by halving the A_T/R_Z ratio where the normalised cross-correlation coefficient is ≥0.8. The *vertical colour bar* between (**d**) and (**i**) indicates the cross-correlation coefficients shown in (**d**) and (**i**), and the *vertical colour bar* between (**e**) and (**j**) shows the velocity distribution (in metres per second) given in the *bottom panels*

signal about the radial axis, immediately after the arrival of the first P-wave, was possibly caused by anisotropy. However, the first P-wave arrival recorded by the R-1 measurements (Fig. 2b) has a much stronger signal than could be reasonably contributed by any anisotropic effects. Thus, the possible contamination of the R-1 measurements by cross-axis rotation is significant, and additional analyses are required to understand these issues. Given that similar results were reported by Nigbor et al. (2009), we do not try to elucidate the results of the R-1-recorded coda waves here. This also explains why we used only the signals of array-derived rotations to analyse scattering effects. Our analysis indicates that signals of rotation about the radial and vertical axes in the time window defined by the first arrival of the P-coda determined by data from the TAIGER experiments might be contributed by the presence of a heterogeneous crustal structure (see Fig. 5).

In summary, we conclude that: (1) rotational motions induced by direct P-waves interacting with a free surface can, in theory, be used to estimate wave radial directions, velocities and anisotropic properties; (2) rotational motions originating from scattering are predominant among observed rotations within data obtained during the TAIGER explosion experiments and allow us to image the heterogeneous structure of the investigated site; and (3) measurements of rotation sensors for the TAIGER explosion experiments may be affected by cross-axis sensitivity; this effect needs to be considered when using those records.

This paper provides new and important information on seismic wave propagation and on the identification of crustal structures using multiple-component point measurements. Below, we suggest a number of issues that remain unclear and that should be addressed in the future:

– As we indicated previously, several phenomena (e.g. anisotropy) can affect direct P-wave rotation amplitudes when interacting with a free surface. We therefore need to consider how the theories presented in this paper (or in Langston and Liang 2008) can be used to estimate wave velocities and what processing steps are required to reduce errors in these estimations.
– In theory, the behaviour of the rotational signal of a direct P-wave on a free surface depends on the direction of origin and the incident angle of the wave. It is necessary to examine whether this rotational signal can help seismologists in the picking of wave phases.
– Can we use direct P-wave-derived rotational signals during inversion to obtain anisotropy parameters?
– With the available observation data, we can follow the methods of Pham et al. (2009a) to constrain the velocity perturbation of the medium at the investigation site; however, it is unclear whether it is possible to go further than this and estimate the correlation length of the medium. If so, what methods should be used?

To clarify these issues, additional observations as well as further numerical modelling are required.

6 Data and resources

The 3D modelling data used in this paper were provided by the Seismology Group at Ludwig Maximilians University, Munich, and have been published by Igel et al. (2005). The observation data obtained during the TAIGER explosion experiments were published by Lin et al. (2009) and are available at the Web page of the International Working Group on Rotational Seismology (http://www.rotational-seismology.org/Members/youngman/papers-and-resources).

Acknowledgments We thank Heiner Igel and other members of the Seismology Group at Ludwig Maximilians University Munich for providing synthetic seismograms. We are grateful to William H.K. Lee and the International Working Group on Rotational Seismology for providing observation data from the TAIGER explosions. Nguyen Dinh Pham, Ngoc-Anh Tran and Tuan-Minh Vu would like to thank the Vietnam National Foundation for Science and Technology Development (NAFOSTED) for financial support through Project 105.04-2010.07. Anonymous reviewers provided helpful comments and suggestions that improved the manuscript.

References

Aki K, Richards PG (1980) Quantitative seismology: theory and methods. W.H. Freeman, San Francisco

Båth M (1979) Introduction to seismology. Birkhauser Verlag, Basel

Bernauer M, Fichtner A, Igel H (2009) Inferring near-receiver structure from combined measurements of rotational and translational ground motions. Geophysics 74(6):WCD41–WCD47

Cochard A, Igel H, Schuberth B, Suryanto W, Velikoseltsev A, Schreiber U, Wassermann J, Scherbaum F, Vollmer D (2006) Rotational motions in seismology: theory, observations, simulation. In: Teisseyre R, Takeo M, Majewski E (eds) Earthquake source asymmetry, structural media and rotation effects. Springer, New York, pp 391–412

eentec (2008) Instruction manual, special case, model R-1 (serial number A200504 thru A200547, St. Louis, Missouri, 8 pp. http://www.eentec.com/. Accessed January 2009

Fichtner A, Igel H (2009) Sensitivity densities for rotational ground motion measurements. Bull Seismol Soc Am 99 (2B):1302–1314

Graizer V (2005) Effect of tilt on strong motion data processing. Soil Dyn Earthq Eng 25:197–204

Graizer V (2006) Tilts in strong ground motion. Bull Seismol Soc Am 96:2090–2102

Gutenberg B (1927) Grundlagen der erdbebenkunde. Univ. Frankfurt a/M

Huang BS (2003) Ground rotational motions of the 1991 Chi-Chi, Taiwan earthquake as inferred from dense array observations. Geophys Res Lett 30(6):1307–1310

Igel H, Schreiber U, Flaws A, Schuberth B, Velikoseltsev A, Cochard A (2005) Rotational motions induced by the M8.1 Tokachi-oki earthquake, September 25, 2003. Geophys Res Lett 32:L08309

Igel H, Cochard A, Wassermann J, Flaws A, Schreiber U, Velikoseltsev A, Pham ND (2007) Broadband observations

of earthquake induced rotational ground motions. Geophys J Int 168:182–196
Langston CA (2007a) Spatial gradient analysis for linear seismic arrays. Bull Seismol Soc Am 97(1B):265–280
Langston CA (2007b) Wave gradiometry in two dimensions. Bull Seismol Soc Am 97:401–416. doi:10.1785/0120060138
Langston CA, Liang C (2008) Gradiometry for polarized seismic waves. J Geophys Res 113:B08305
Langston CA, Lee WHK, Lin CJ, Liu CC (2009) Seismic-wave strain, rotation, and gradiometry for the 4 March 2008 TAIGER explosions. Bull Seismol Soc Am 99(2B):1287–1301
Lay T, Wallace TC (1995) Modern global seismology. Academic, San Diego
Lee WHK, Celebi M, Todorovska MI, Igel H (2009a) Introduction to the special issue on rotational seismology and engineering applications. Bull Seismol Soc Am 99(2B):945–957
Lee HKW, Igel H, Trifunac MD (2009b) Recent advances in rotational seismology. Seismol Res Lett 80(3):479–490
Li H, Sun L, Wang S (2001) Improved approach for obtaining rotational components of seismic motion. Trans, SmiRT 16:1–8
Liang C, Langston CA (2009) Wave gradiometry for USArray: Rayleigh waves. J Geophys Res 114:B02308. doi:10.1029/2008JB005918
Lin CJ, Liu CC, Lee WHK (2009) Recording rotational and translational ground motions of two TAIGER explosions in northeastern Taiwan on 4 March 2008. Bull Seismol Soc Am 99(2B):1237–1250
Lin CJ, Huang HP, Pham ND, Liu CC, Chi WC, Lee WHK (2011) Rotational motions for teleseismic surface waves. Geophys Res Lett 38:L15301
Lin CJ, Huang WG, Huang HP, Huang BS, Ku CS, Liu CC (2012) Investigation of array derived rotation. J Seismol (this volume)
McLeod DP, Stedman GE, Webb TH, Schreiber U (1998) Comparison of standard and ring laser rotational seismograms. Bull Seismol Soc Am 88:1495–1503
Metrozet LLC (2007) Triaxial seismic accelerometer TSA-100S: user's manual, Torrance, California. http://www.metrozet.com/. Accessed January 2009
Nigbor RL, Evans JR, Hutt CR (2009) Laboratory and field testing of commercial rotational seismometers. Bull Seismol Soc Am 99(2B):1215–1227
Okaya D, Wu FT, Wang CY, Yen HY, Huang BS, Brown L, Liang WT (2009) Joint passive/controlled source seismic experiment across Taiwan. Eos 90:289–290
Pancha A, Webb TH, Stedman GE, McLeod DP, Schreiber U (2000) Ring laser detection of rotations from teleseismic waves. Geophys Res Lett 27:3553–3556
Pham DN, Igel H, Wassermann J, Käser M, de la Puente J, Schreiber U (2009a) Observations and modelling of rotational signals in the P-coda: constraints on crustal scattering. Bull Seismol Soc Am 99(2B):1315–1332
Pham DN, Igel H, Wassermann J, Cochard A, Schreiber U (2009b) The effects of tilt on interferometric rotation sensors. Bull Seismol Soc Am 99(2B):1352–1365
Pham DN, Igel H, de la Puente J, Käser M, Schoenberg MA (2010) Rotational motions in homogeneous anisotropic elastic media. Geophysics 75:D47–D56
Pillet R, Virieux J (2007) The effects of seismic rotations on inertial sensors. Geophys J Int 171:1314–1323
Richter CF (1958) Elementary seismology. W.H. Freeman, San Francisco
Schreiber U, Igel H, Cochard A, Velikoseltsev A, Flaws A, Schuberth B, Drewitz W, Müller F (2005) The GEOsensor Project: a new observable for seismology. In: Flury J, Rummel R, Reigber C, Rothacher M, Boedecker G, Schreiber U (eds) Observation of the System Earth from space. Springer, Berlin, pp 427–443
Schreiber U, Stedman GE, Igel H, Flaws A (2006) Ring laser gyroscopes as rotation sensors for seismic wave studies. In: Teisseyre R, Takeo M, Majewski E (eds) Earthquake source asymmetry, structural media and rotation effects. Springer, New York, pp 377–390
Spudich P, Fletcher JB (2008) Observation and prediction of dynamic ground strains, tilts, and torsions caused by the *M*w 6.0 2004 Parkfield, California, earthquake and aftershocks, derived from UPSAR array observations. Bull Seismol Soc Am 98(4):1898–1914
Suryanto W, Igel H, Wassermann J, Cochard A, Schuberth B, Vollmer D, Scherbaum F, Schreiber U, Velikoseltsev A (2006) First comparison of array-derived rotational ground motions with direct ring laser measurements. Bull Seismol Soc Am 96(2):2059–2071. doi:10.1785/0120060004
Trifunac MD, Todorovska IM (2001) A note on the usable dynamic range of accelerographs recording translation. Soil Dyn Earthq Eng 21(4):275–286
Wu FT, Liang WT, Lee JC, Benz H, Villasenor A (2009) A model for the termination of the Ryukyu subduction zone against Taiwan: a junction of collision, subduction/separation, and subduction boundaries. J Geophys Res 114:B07407